Synthesis, Photodegradation, and Energy Transfer in a Series of Poly(ethylene Terephthalate-*co*-2,6-Naphthalenedicarboxylate) Copolymers

PING-SUN R. CHEUNG and CARLETON W. ROBERTS, *Textile Department, Clemson University, Clemson, South Carolina 29631,* and KENNETH B. WAGENER, *Akzona Inc., Enka, North Carolina 28728*

Synopsis

Triplet–triplet energy transfer has been shown to occur from poly(ethylene terephthalate) (PET) units to the 2,6-naphthalenedicarboxylate (2,6-ND) monomer units in a series of poly(ethylene terephthalate-*co*-2,6-naphthalenedicarboxylate) (PET–2,6-ND) copolymers, as filament yarns, by an exchange mechanism at 77°K. The radius of the "quenching sphere" has been calculated to be 19.7 Å, indicating the presence of triplet energy migration. Photostabilization was observed in the copolymer yarns with the concentration of the monomer dimethyl 2,6-naphthalenedicarboxylate (2,6-DMN) at or above 2 mol %; the rate of phototendering in an air atmosphere was shown to decrease from 2.0×10^{-19}% breaking strength loss/quantum absorbed/cm^2 in the homopolymer PET to 0.7×10^{-19}% breaking strength loss/quantum absorbed/cm^2 in the copolymer yarns. The photophysical processes in the monomers, dimethyl terephthalate and 2,6-DMN, were examined by absorption and luminescence studies. The lowest excited singlet and triplet in both monomers were identified to be the $^1(\pi,\pi^*)$ and $^3(\pi,\pi^*)$ states, respectively. The phosphorescence of PET was shown to originate from a $^3(\pi,\pi^*)$ state, while the complex fluorescence spectrum may arise from some oriented aggregates in the polymer matrix. In copolymer yarns, only the fluorescence emission from the 2,6-ND monomer units at 380 nm was observed. The phosphorescence spectra of the copolymer yarns showed phosphorescence emissions from the PET and 2,6-ND monomer units; in addition, delayed fluorescence from the 2,6-ND monomer was also observed.

INTRODUCTION

Although poly(ethylene terephthalate) (PET) displays reasonably good resistance toward sunlight, it is susceptible to photodegradation on long-term exposure to the ultraviolet radiation of terrestrial sunlight resulting in a loss of desirable physical properties and changes in chemical properties. The photodegradation of PET has been related to the presence of energy-absorbing groups, the aromatic ester groups, in the polymer backbone.[1] On exposure to sunlight, PET fibers tend to lose their tenacity, elongation, and elasticity, and PET films become discolored, brittle, and develop a crazed surface. PET has been shown to absorb radiation strongly below 315 nm but is transparent to radiation greater than 320 nm.[2] The photodegradation processes in the polymer are affected by the wavelength and intensity of the radiation, the radiation atmosphere, and the presence or absence of additives such as dyes and delustrants. Many reports on various aspects of photodegradation of PET have been published.[1–10]

The photochemical degradation of PET film has been extensively investigated, and both the physical and chemical changes were measured as a function of irradiation time. Recent thorough studies of the photochemical degradation of

Journal of Applied Polymer Science, Vol. 24, 1809–1830 (1979)

0021-8995/79/0024-1809$01.00

PET by Day and Wiles[11–14] led to the postulation of the mechanisms for primary photodegradation processes. The understanding of the mechanisms for photodegradation processes is of vital importance in the improvement of the photostabilization of the polymer.

Usually, polymers are protected against photodegradation by addition of photostabilizers. The stabilizers are generally divided into three groups: light screens, ultraviolet absorbers, and quenching compounds. Photostabilizers of low molecular weight may migrate from the polymers during storage and may also evaporate during the molding and extrusion processes. The modification of polymer structure to improve the photostabilization of the polymer is an important but somewhat neglected method. Stabilizers can be incorporated in the structure during polymerization or grafted onto the polymer in a subsequent reaction to form a copolymer.

The quenching effects of photostabilizers can be explained by the mechanism of energy transfer between an excited polymer molecule and a photostabilizer. Several theoretical treatments for nonradiative energy transfer have been developed. The energy transfer mechanisms have been explained based on dipole–dipole interactions,[15–19] electron exchange interactions,[20–22] and exciton migration.[23,24] Energy transfer in polymer systems has been studied extensively by David et al.[25–31] and recently reviewed by Turro[32] and Guillet.[33] It is generally assumed that the concepts of energy transfer processes to small molecules in solution can be applied to the chromophores in polymer systems. The characteristics of the polymer system in solid form are the lack of molecular conformation of the polymer backbone and also the pendant groups. But the presence of the repeat structural units enables the formation of domains which are crystalline in nature, and this may favor the energy migration processes.

Although the photophysical processes in many polymers, copolymers, and polymer–additive mixtures have been studied extensively,[34–36] few investigations of the photophysical phenomena in aromatic esters have been reported. Several research groups have studied the luminescence behavior of PET and diverse results were reported in the literature. Cheung[37] has studied the photophysical processes of three model esters of PET; the observed fluorescence and phosphorescence from the aromatic esters were tentatively assigned as $^1(n,\pi^*)$ and $^3(\pi,\pi^*)$ transitions, respectively. Merrill and Roberts[10] studied the luminescence of PET fiber and film; they also proposed a $^1(n,\pi^*)$ transition for the fluorescence emission and a $^3(\pi,\pi^*)$ transition for the phosphorescence emission from the PET polymer. However, a recent study by Allen and McKellar[38] suggested that the fluorescence from PET polymer may be due to the emission from associated ground-state dimers.

In this research, copolyesters containing terephthalate and 2,6-naphthalenedicarboxylate moieties were synthesized. The photophysical processes of the monomers dimethyl terephthalate and dimethyl 2,6-naphthalenedicarboxylate, the homopolymer PET, and the copolyesters were studied. The energy transfer processes were examined in the copolyester systems and were related to the rates of phototendering in the homopolymer and copolymer. The extent of phototendering was assessed by measuring the percent loss in yarn breaking strength as a function of total incident radiation.

EXPERIMENTAL

Materials and Analyses

Dimethyl 2,6-naphthalendicarboxylate was purchased from Aldrich Chemical Company. Dimethyl terephthalate and 1,1,1,3,3,3-hexafluoro-2-propanol (HFIP) were obtained from Eastman Organic Chemicals. Certified ACS-grade acetonitrile, ferric ammonium sulfate, ferrous ammonium sulfate, potassium oxalate, 1,10-phenanthroline (monohydrate), and sodium acetate were obtained from Fisher Scientific Company. USP-grade 95% ethanol, after further purification, was used for luminescence studies. Nuchar granular activated carbon (12 × 40 mesh) was used to remove colored impurities from the dimethyl 2,6-naphthalenedicarboxylate.

Ultraviolet absorption spectra were obtained from a Cary 118C spectrophotometer. Luminescence measurements were obtained from a Perkin–Elmer Model MPF-3 fluorescence spectrophotometer equipped with corrected spectra, phosphorescence, and front surface accessories. A Tektronix Model 5103N storage oscilloscope was used for luminescence lifetime measurements. Photolyses were carried out in a Rayonet Type RS Model RPR-208 preparative photochemical reactor equipped with a MGR-100 merry-go-round assembly. Yarn samples were knit on a Lawson fiber analysis knitter (FAK). Yarn tensile testing was performed on an Instron Model 1101 (TM-M) constant rate of extension testing machine.

Purification of Dimethyl Terephthalate (DMT)

Dimethyl terephthalate was twice recrystallized from 95% ethanol (1:25) to give white needle-like crystals, mp 141–142°C.

Purification of Dimethyl 2,6-Naphthalenedicarboxylate

Crude dimethyl 2,6-naphthalenedicarboxylate was recrystallized with decolorization from acetonitrile (1:80), and the white, dried product was recrystallized twice from 95% ethanol (1:100) to give pure product, mp 189–190°C.

Synthesis of Copolyesters Containing Dimethyl 2,6-Naphthalenedicarboxylate

Copolymers were prepared from dimethyl terephthalate containing 0.5, 1, 2, or 4 mol % dimethyl 2,6-naphthalenedicarboxylate and 2.3 moles ethylene glycol per mole diesters. A typical preparation follows.

Dimethyl terephthalate, ethylene glycol, and dimethyl 2,6-naphthalenedicarboxylate were charged into a 1-kg resin kettle equipped with a mechanical stirrer, a nitrogen inlet tube, a thermocouple attached to a Barber–Coleman recorder, a dual partial condenser with the lower column being heated to 130°C by a circulating oil bath and the upper column being heated at 70°C by a circulating hot water bath, and an automatic reflux ratio distillation head mounted above the column. Just prior to heating, 0.03 mol % (based on DMT) manganese acetate was added to the reaction mixture. A continuous nitrogen purge was begun, and the resin kettle was brought to 120°C with a heating mantle; at this

time, low-speed stirring was initiated. The temperature was allowed to rise to 215°C over an hour, during which time the theoretical quantity of methanol was collected as distillate. At about 180°C, where the ester exchange reaction usually began, 0.05 mol % (based on DMT) antimony oxide was added along with triphenyl phosphate designed to complex the ester interchange catalyst, manganese.

After the reaction was completed, the colorless liquid was poured into a polymerization vessel designed for high-torque stirring under high vacuum and the vessel was then mounted to a stirrer unit. The vessel was heated with a dimethyl phthalate boiler, and a vacuum program was initiated. The stirring rate was set at 300 rpm, continued through the polycondensation process, and eventually reduced to 75 rpm. During this period, which lasted for approximately 2 hr, ethylene glycol was distilled and collected. The polymer was then extruded into a water bath, dried, and submitted for intrinsic viscosity, acid, and phosphorous content determinations.

Characterization of Copolyesters

For intrinsic viscosity determination, a 0.18-g polymer sample was dissolved in phenol tetrachloroethane (40:60) (1.0 wt-% solution) and heated to 90°C for 2 hr. The solution was transferred to a Ubbelhode viscometer in a constant-temperature bath (25° ± 0.1°C) and the emergent flow times T_S were measured. The flow time of the solvent, T_0, was measured similarly. The relative viscosity was determined as $\eta_{rel} = T_S/T_0$ and was converted to intrinsic viscosity by

$$[\eta] = \frac{\eta_{rel} - 1 + 3(\ln \eta_{rel})}{4}$$

The above relation assumed identical slopes for PET solutions when plotting η_{rel}/C versus C, where C is the solution concentration.

For phosphorus content determination, a polymer sample containing not more than 0.13 mg PO_4^{3-} was weighed in a platinum dish, and 2 ml saturated NaCl solution was added prior to evaporating the mixture to dryness. The residue was ashed at ~600°C for ~15 min. The ash was cooled, mixed with 5 ml concentrated HCl for 5 min, and transferred quantitatively to a 25-ml volumetric flask. The solution was diluted to 20 ml with distilled water followed by the addition of 1.0 ml molybdate–tartrate reagent and 1.0 ml ANSA reagent and then brought to 25 ml by addition of distilled water. The absorbance of this solution at 420 nm was measured against a blank, and the ppm phosphate was calculated by

$$\frac{\text{absorbance} \times \text{factor}}{\text{sample weight}} = \text{ppm } PO_4^{3-}$$

The "factor" was determined routinely by measuring known concentrations of PO_4^{3-}.

For acid number determination, a method similar to that described by Pohl[39] was used.

The results of characterization of amorphous copolyesters and crystalline copolyester yarns are shown in Tables I and II.

TABLE I
Characterization of Amorphous Copolyester Polymers

2,6-ND in feed, mol %	I.V.[a]	Acid[b] no.	Phosphorus[c] ppm	T_{cc}[d]	Tm[d]	T_{rc}[d]	T_{rm}[d]
0.0	0.57	10	39	125	254	208	254
0.5	0.61	14	58	—	252	210	—
1.0	0.55	32	82	134	253	206	253
2.0	0.59	11	59	136	251	208	252
4.0	0.58	11	51	145	247	188	247

[a] Intrinsic viscosity, measured in 40% phenol/60% tetrachloroethane.
[b] Equals Meq/kg polymer.
[c] Based on weight of polymer.
[d] DTA measurements, point of curve maximum (or minimum); T_{cc} = cold crystallization temperature; T_m = melting temperature; T_{rc} = recrystallization temperature; T_{rm} = remelt temperature.

Preparation and Irradiation of Copolymer Yarns

The multifilament yarns were knit into a tubular form to facilitate handling during the scouring process. The tubular knit yarn samples were scoured at 75–80°C for 20 min with a 5% (by weight) aqueous solution of tetrasodium pyrophosphate (TSPP) in a liquor ratio of 50:1. The samples were then cooled, removed, rinsed with distilled water, and air dried. The knit yarn samples were unraveled and mounted on a wire frame (41 × 3 cm). Irradiation conditions were similar to those described previously.[10]

Yarn-Breaking Strength

The yarn-breaking strength was determined as previously described.[10]

Actinometry

The light intensity of the 3000-Å irradiating lamps and the lamp's-aging effect were monitored using potassium ferrioxalate chemical actinometer developed by Hatchard and Parker[40,41] and modified by Baxendale and Bridge,[42] Lee and Seliger[43] Kurien,[44] and Nicodem, Cabral, and Ferreira.[45] The lamp intensities were found to decrease from a maximum of 1.08×10^{15} quanta/cm^2-sec to 0.89

TABLE II
Characterization of Crystalline Copolyester Yarns (30/6)

2,6-ND in feed, mol %	T_m[a]	T_{rc}[a]	T_{rm}[a]	Denier	Tenacity, g/den	Elongation, %	Toughness, g-cm/den
0.0	257	220	252	30.4	3.1 ± 0.3	16 ± 5	10 ± 3
0.5	255	214	251	33.2	1.9 ± 0.1	13 ± 8	4.4 ± 3
1.0	254	216	250	36.6	2.7 ± 0.1	13 ± 1	6.6 ± 0.7
2.0	254	208	247	31.1	3.1 ± 0.2	12 ± 2	6.4 ± 1.3
4.0	247	206	245	37.0	2.7 ± 0.1	29 ± 2	15 ± 1.3

[a] DTA measurements, point of curve maximum (or minimum); T_m = melting temperature; T_{rc} = recrystallization temperature; T_{rm} = remelt temperature.

$\times 10^{15}$ quanta/cm^2-sec, measured at 9.2 cm from the surface of the lamps, after 800 hr.

RESULTS AND DISCUSSION

Photophysical Processes in Dimethyl Terephthalate (DMT)

The absorption spectra of dimethyl terephthalate in HFIP and 95% ethanol were measured between 180 and 400 nm. In HFIP solution, dimethyl terephthalate displayed three absorption bands at about 191, 244, and 289 nm, which can be assigned to the $^1A \rightarrow {}^1B$, $^1A \rightarrow {}^1L_a$, and $^1A \rightarrow {}^1L_b$ transitions, respectively; in ethanol solution, only two bands, at 241 and 286 nm, were observed (Table III).

The corrected excitation and fluorescence spectra of dimethyl terephthalate in HFIP at 298°K displayed band maxima for the excitation spectrum at 248 and 290 nm; in addition, an emission spectrum exhibited a structureless band with a maximum at 322 nm. Similar excitation and fluorescence spectra of dimethyl terephthalate were observed in 95% ethanol, but the emission from DMT in ethanol solution was about 100 times less intense as that in HFIP solution. The very low-intensity fluorescence from dimethyl terephthalate in ethanol solution is expected, and it has been observed from analogous compounds such as methyl benzoate and benzoic acid.[46]

In Figure 1 are presented uncorrected phosphorescence excitation and emission spectra of dimethyl terephthalate in 95% ethanol at 77°K. Excitation band maxima were observed at 252 and 298 nm, while an intense emission spectrum exhibited a structured band with maxima at 391, 404, 418, 432, and 446 nm and a mean lifetime (τ) of 2.2 sec.

The structured phosphorescence emission band centered at 418 nm is most likely from a ^3L_a (π,π^*) state as evidenced by the long phosphorescence lifetime, ~2.2 sec, and the large $^1S_2$–$^3T_1$ energy splitting, 16,000 cm^{-1}.[35] Similar phosphorescence bands have been observed in benzoic acid, methyl benzoate,[46] and terephthalic acid.[47] From the vibrational analysis of the phosphorescence band, the frequency ~800 cm^{-1} can be attributed to the out-of-plane bending of the aromatic ring.[48]

The low-intensity fluorescence and strong phosphorescence of dimethyl terephthalate can be explained by assuming that the $^3(n,\pi^*)$ state is located below the ^1L_b state. It has been shown by El-Sayed[49] that, to a first-order approxi-

TABLE III
Absorption Characteristics of Dimethyl Terephthalate

Solvent	λ, nm	ε, l/cm mol
Hexafluoroisopropanol	191.0	40,620
	244.0	23,880
	289.0	1,780
	297.0 (s)[a]	1,379
95% Ethanol	241.2	20,630
	286.2	2,074
	294.0 (s)[a]	1,298

[a] Shoulder.

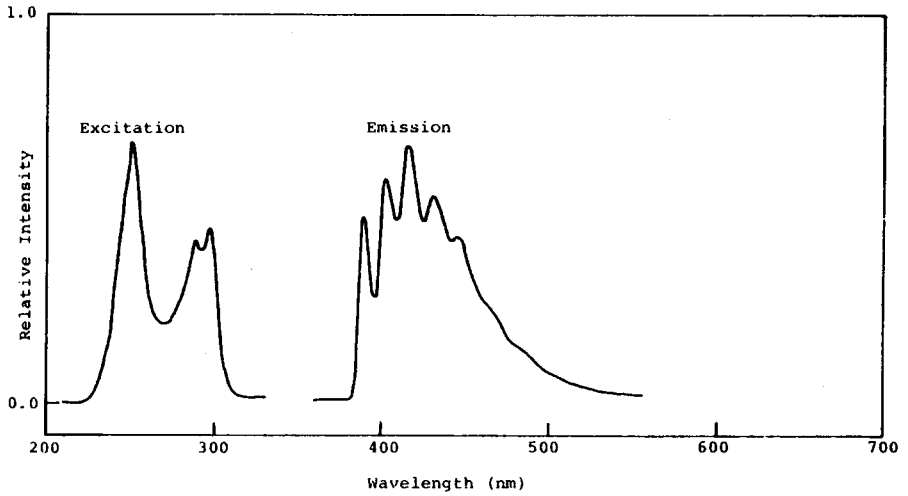

Fig. 1. Uncorrected phosphorescence excitation and emission spectra of dimethyl terephthalate ($5 \times 10^{-5} M$) in 95% ethanol at 77°K. Excitation scan: Em λ 418 nm; emission scan: Ex λ 250 nm; lifetime (τ) 2.2 sec.

mation, spin-orbit coupling between $^1(\pi,\pi^*)$ and $^3(n,\pi^*)$ states is 10^3 times larger than that between $^1(\pi,\pi^*)$ and $^3(\pi,\pi^*)$ states. Therefore, dimethyl terephthalate will become nonfluorescent or weakly fluorescent but strongly phosphorescent due to the efficient spin-orbit coupling between $^1(\pi,\pi,^*)$ and $^3(n,\pi^*)$ states which leads to a high rate of intersystem crossing, $^1L_b \rightarrow {}^3(n,\pi^*)$. However, in a more polar solvent such as HFIP, the energy level of the $^3(n,\pi^*)$ state is raised, as in the case of the $^1(n,\pi^*)$ state, because of stronger hydrogen bonding. In this case, we assume that the $^3(n,\pi^*)$ level is higher than the ^1L_b in HFIP solution. Since the spin-orbit interaction between $^1(\pi,\pi^*)$ and $^3(\pi,\pi^*)$ states is very small, the rate of intersystem crossing, $^1L_b \rightarrow {}^3L_a$, is low enough for the fluorescence transition to compete with the intersystem crossing, resulting in rather strong fluorescence in HFIP solution.

The 0–0 transition bands from the fluorescence and phosphorescence spectra of dimethyl terephthalate yield the following electronic state energies: $^1S_1 \sim 33{,}000\ cm^{-1}$, $^1S_2 \sim 42{,}000\ cm^{-1}$, and $^3T_1 \sim 26{,}000\ cm^{-1}$. The electronic energy diagram of dimethyl terephthalate and the band assignments are shown in Figure 2.

Photophysical Processes in Dimethyl 2,6-Naphthalenedicarboxylate (2,6-DMN)

The UV absorption spectra of dimethyl 2,6-naphthalenedicarboxylate (2,6-DMN) in HFIP and 95% ethanol were measured between 200 and 400 nm. In this region, similar absorptions were obtained in both solvent systems; three bands at about 243, 295, and 350 nm corresponding to $^1A \rightarrow {}^1B_b$, $^1A \rightarrow {}^1L_a$, and $^1A \rightarrow {}^1L_b$ transitions were observed. Figure 3 presents the absorption spectra of 2,6-DMN in HFIP. The absorption spectrum of 2,6-DMN agrees with the results reported by Phillips and Schug.[50]

The corrected excitation and fluorescence spectra of 2,6-DMN in HFIP at 298°K showed excitation maxima at 244, 293, and 355 nm, while an intense emission spectrum exhibited a band maximum at 380 nm.

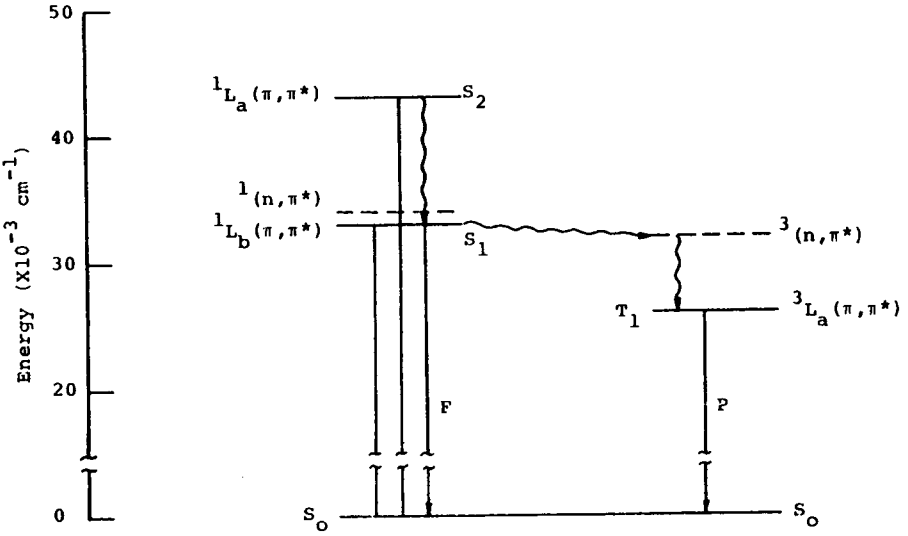

Fig. 2. Electronic energy level diagram and transitions for dimethyl terephthalate in ethanol solution. Estimated levels are represented by broken lines.

The uncorrected excitation and phosphorescence spectra of a rigid glass solution of 2,6-DMN in 95% ethanol at 77°K showed band maxima for the excita-

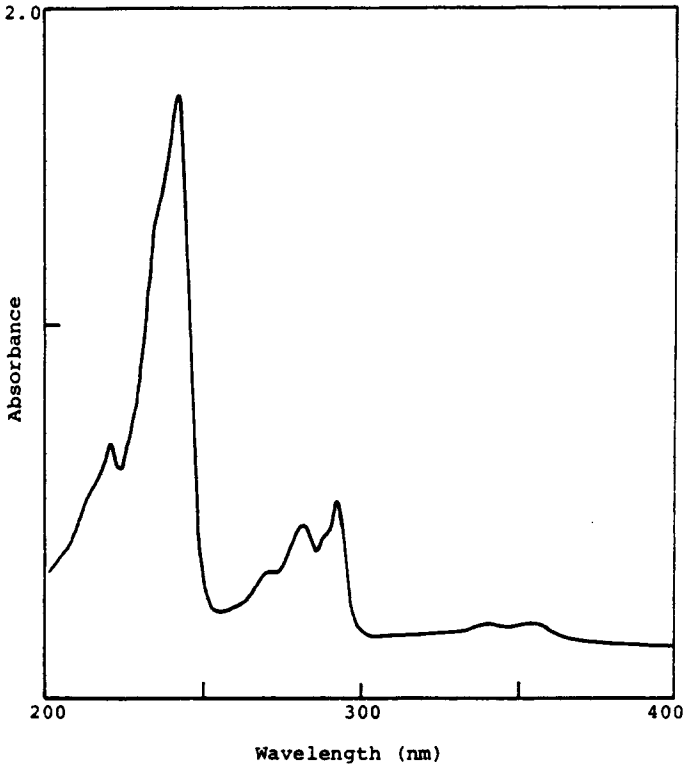

Fig. 3. Absorption spectrum of $2 \times 10^{-5}M$ solution of dimethyl 2,6-naphthalenedicarboxylate in hexafluoroisopropanol.

tion at 250, 296, and 352 nm, while a very weak phosphorescence emission exhibited a structured band with maxima at 500 and 540 nm and a mean lifetime (τ) of 2.0 sec.

Information on the luminescence behavior of naphthalene-derived carboxylic acids and esters are scarce.[51–53] It has been reported that the 2-substituted naphthoic acids and amides exhibit strong fluorescence but very weak phosphorescence.[54] Similar luminescence characteristics were observed in 2,6-DMN where a strong fluorescence emission at about 380 nm and a very weak phosphorescence emission system appeared in the 500–550 nm region. It appears that the $^1(n,\pi^*)$ and $^3(n,\pi^*)$ states in 2,6-DMN are at higher energy levels than the ^1L_b (π,π^*) state (see Fig. 4). Since the spin-orbit interaction between $^1(\pi,\pi^*)$ and $^3(\pi,\pi^*)$ states is very small, the rate of intersystem crossing is low, and strong fluorescence is observed.

Although the fluorescence emission system at 380 nm agrees with the results reported by Phillips and Schug,[50] the phosphorescence emission system starting at 600 nm reported by Phillips has not been observed. However, a very weak phosphorescence emission system around 500 nm was noted at 77°K. It appears that the emission system at 600 nm reported by Phillips could be due to some impurities. The phosphorescence band observed in this study is probably from a ^3L_a (π,π^*) state; this is supported by the long phosphorescence lifetime, ~2.0 sec, and the large $^1S_2$–$^3T_1$ energy splitting, ~15,000 cm^{-1}.[35]

The 0–0 transition bands from fluorescence and phosphorescence spectra of 2,6-DMN yield the following electronic state energies: $^1S_1 \sim 29{,}000$ cm^{-1}; $^1S_2 \sim 35{,}000$ cm^{-1}; $^1S_3 \sim 41{,}000$ cm^{-1}; and $^3T_1 \sim 20{,}000$ cm^{-1}. The electronic energy diagram and the band assignments of 2,6-DMN are shown in Figure 4.

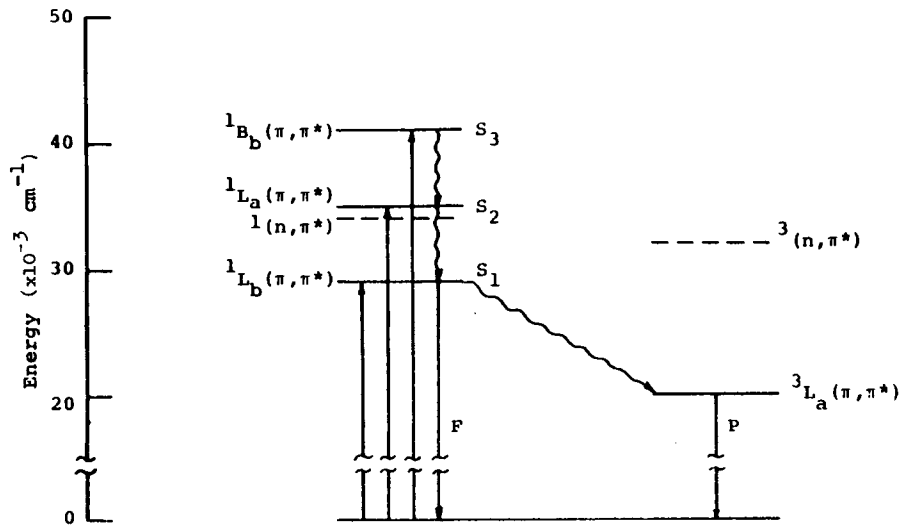

Fig. 4. Electronic energy level diagram and transitions for dimethyl 2,6-naphthalenedicarboxylate in ethanol solution. Estimated levels are represented by broken lines.

Photophysical Processes in Poly(ethylene Terephthalate) (PET)

The room-temperature electronic absorption spectrum of PET in HFIP solution is shown in Figure 5. The absorption spectrum consists of three bands appearing at about 291, 245, and 191 nm, which can be assigned to $^1A \rightarrow {}^1L_b$, $^1A \rightarrow {}^1L_a$, and $^1A \rightarrow {}^1B$ transitions, respectively.

The electronic absorption spectra of PET films of various thicknesses have been reported.[1,11,55] The absorption spectrum of PET in HFIP solution (Fig. 5) agrees well with the results reported by Marcotte et al.[1] and Takai et al.[55] The absorption bands at 291, 245, and 191 nm are most likely $^1(\pi,\pi^*)$ transitions which correspond to the $^1A \rightarrow {}^1L_b$, $^1A \rightarrow {}^1L_a$, and $^1A \rightarrow {}^1B$ transitions in DMT. In DMT, these transitions were shown to occur at 286, 241, and 191 nm, respectively.

The corrected fluorescence excitation and emission spectra of PET in HFIP solution at 298°K showed band maxima for the excitation at 255 and 292 nm and emission at 325 nm.

The corrected fluorescence excitation and emission spectra of PET yarns at 298°K showed structured excitation band centered at 342 nm and a similar emission band centered at 390 nm. The similarities between the fluorescence excitation and emission spectra of PET and DMT in HFIP solution indicate that the excitation and emission of PET in HFIP solution originate from the monomer units.

The uncorrected phosphorescence excitation and emission spectra of PET

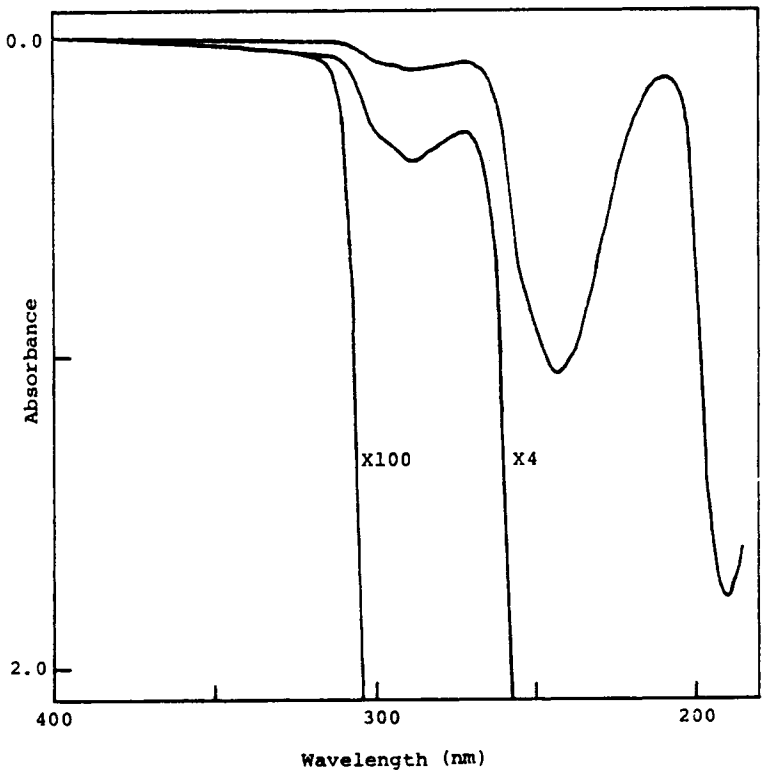

Fig. 5. Absorption spectrum of 9.4 × 10^{-4} g/100 ml poly(ethylene terephthalate) in hexafluoroisopropanol.

yarns at 77°K showed an excitation emission maximum at 312 nm and a broad, structureless emission band centered at 452 nm with a mean lifetime (τ) of 1.2 sec. The phosphorescence emission band at 452 nm agrees with the results reported by Allen et al.[56] and Merrill and Roberts.[10] The emission is most likely from a $^3(\pi,\pi^*)$ state on account of the long phosphorescence lifetime, ~1.2 sec, and large S_2–T_1 energy splitting, ~14,000 cm^{-1}.

The fluorescence excitation and emission bands of PET yarn, at 342 and 390 nm, respectively, have been reported by many research groups.[8,10,11,56] It is generally agreed that the luminescence originates from the polymer itself and not from impurities, because similar luminescence properties have been observed from various forms of PET polymer such as polymer chips, films, and yarns produced by different manufacturers.

Band assignments for the polymeric species are very difficult because of the complex structure of the polymer. There has been controversy on the origin of PET fluorescence at 390 nm ever since an early study of PET luminescence by high-energy electron excitation.[50] Phillips and Schug[50] suggested that the broad emission band at 390 nm may arise from the triplet state or an excimer state. Since it has been shown that PET and its model compound DMT have a triplet state of much lower energy, ~450 nm, the emission band at 390 nm is unlikely from a triplet state. Also, if an excimer is formed by the interaction of an excited molecule and a ground-state molecule of the same kind, there should not be a change in the excitation spectra between the monomer and excimer. Hence, the emission band at 390 nm is unlikely to have arisen from an excimer state.

Since the excitation band at 310 nm for PET phosphorescence has been assigned as a $^1(\pi,\pi^*)$ transition, the excitation band at 340 nm for PET fluorescence was suggested to arise from a $^1(n,\pi^*)$ state by Merrill and Roberts.[10] However, from the analysis of luminescence of the model compound DMT, and with similar arguments presented for the model compound, the $^1(n,\pi^*)$ state in PET yarn is probably hidden under the strong $^1(\pi,\pi^*)$ transition and is possibly at a higher energy level than the $^1(\pi,\pi^*)$ transition. Therefore, the PET fluorescence at 390 nm is also unlikely due to a $^1(n,\pi^*)$ state.

From the luminescence study of high concentration of PET in trifluoroacetic acid, Allen and McKellar[38] reported that a low concentrations of PET (i.e., ~5 g/l.), only monomer fluorescence was observed at 330 nm. At concentrations between 5 and 25 g/l., they observed that the excitation maximum was red-shifted from 290 to 340 nm and emission band was observed with wavelength maxima at 460 and 392 nm. At even higher concentrations of PET (i.e., ~50 g/l.), the fluorescence emission gave a broad, structureless band centered at 460 nm. Based on these observations, Allen and McKellar suggested that dimerization occurs in concentrated solution of PET and that the emission band at 392 nm observed in solid polymer is due to associated ground-state dimer fluorescence.

The absorption and luminescence behavior of PET in HFIP at high concentrations have been studied. No evidence has been found in the absorption and fluorescence excitation and emission spectra (Fig. 6), even at high concentration (25 g/l.), which would indicate the existence of a stable ground-state dimer. In all cases, the monomer fluorescence at about 325 nm was observed, and the excitation maxima were displaced to longer wavelengths at high concentrations due to the inner-filtering effect.

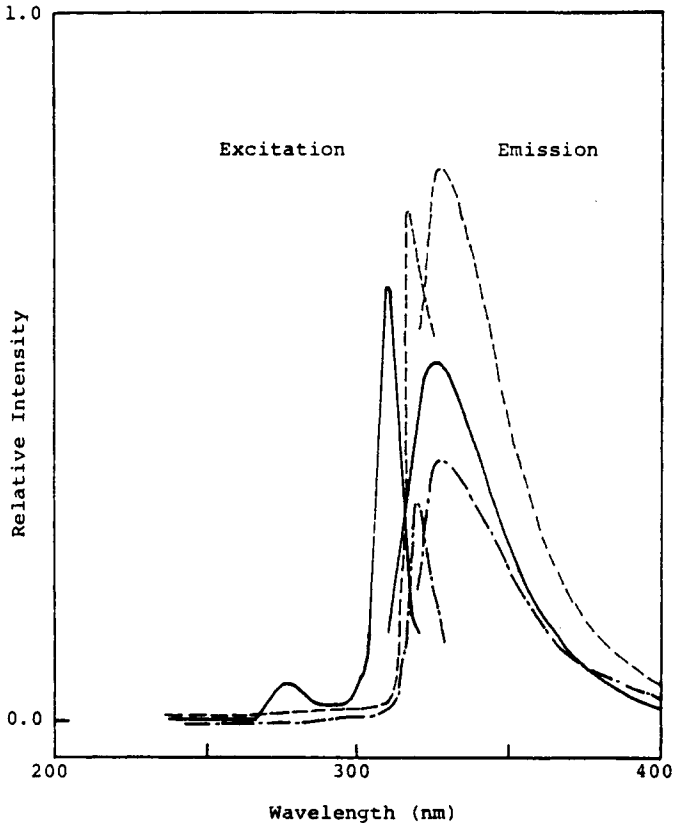

Fig. 6. Corrected fluorescence excitation and emission spectra of poly(ethylene terephthalate) in hexafluoroisopropanol at 298°K: (—) 0.8 g/l; (---) 11 g/l; (-·-) 25 g/l. Excitation scan: Em λ 325 nm; emission scan: Ex λ 310 nm.

There is uncertainty whether the excitation and emission observed at 340 and 390 nm, respectively, in high concentrations of PET in trifluoroacetic acid are originating from the gound-state dimer. The repulsive nature between benzene moieties makes the dimerization process unfavorable in solution, and the luminescence observed from PET in trifluoroacetic acid may possibly arise from the complex formation between the solvent and the ester groups in the polymer backbone.

Fluorescence emission from PET at other wavelengths has also been reported.[57,58] Padhyde and Tamhane[57] reported fluorescence emission at 304, 326, and 365 nm from PET films at 77°K. They suggested that these fluorescence bands arise from different environments. Takai, Mizutani, and Ieda[58] reported emission bands at 335 and 365 nm from PET films when excited at 280 nm. They suggested that the 335 nm emission band originates from monomer emission while the 365 nm band arises from excimer emission.

The structured fluorescence spectra of PET suggest that the emitting chromophores are fixed in specific geometry in the polymer matrix. Thus, the PET fluorescence would appear to arise from aggregates of monomeric units fixed in specific geometry in the polymer matrix, and the fluorescence is analogous to the crystal emission observed in many organic crystals.

The 0–0 bands for PET fluorescence in HFIP and PET yarn phosphorescence yield the following electronic state energies: $S_1 = 32{,}600\ cm^{-1}$; $S_2 = 39{,}000\ cm^{-1}$; $T_1 = 25{,}000\ cm^{-1}$. The O–O band for PET fluorescence (possibly arising from oriented aggregates) yields $S_1' = 27{,}000\ cm^{-1}$. The electronic energy diagram and band assignments of PET are shown in Figure 7.

Photophysical Processes in Poly(ethylene Terephthalate–*co*–2,6-Naphthalenedicarboxylate) (PET–2,6-ND)

The PET–2,6-ND copolymers, with concentrations of 2,6-DMN ranging from 0.5 to 4.0 mol %, have UV absorption spectra similar to that of the PET homopolymer in HFIP solution. Absorption bands were observed at about 191, 245, and 291 nm. The absorption band structure in the 291-nm region starts to change with increasing concentration of 2,6-DMN monomer; increased absorption in the 350-nm region was also observed. The band assignments for the absorption spectra of the copolymer correspond to those in the homopolymer PET and the monomer 2,6-DMN.

Although the presence of naphthalendicarboxylate (ND) monomer is barely observable in the absorption spectra of the copolymer (because of its low concentration), its existence is distinctly displayed in the fluorescence and emission spectra. The corrected fluorescence excitation and emission spectra of some of the PET-2,6-ND copolymers in HFIP solution are shown in Figure 8. The band maxima for the excitation spectra of the copolymer were observed at about 355, 295, and 247 nm and the fluorescence emission shows maxima at 325, 372, and 390 nm. The emission intensity at 390 nm, which originates from the naphthalenedicarboxylate units, increases with 2,6-DMN concentration in the copolymer. A linear correlation was obtained when plotting the fluorescence intensities of the copolymers in HFIP solution versus the concentrations of 2,6-DMN in the copolymer.

Figure 9 shows some of the fluorescence spectra of the copolymer yarns. Broad

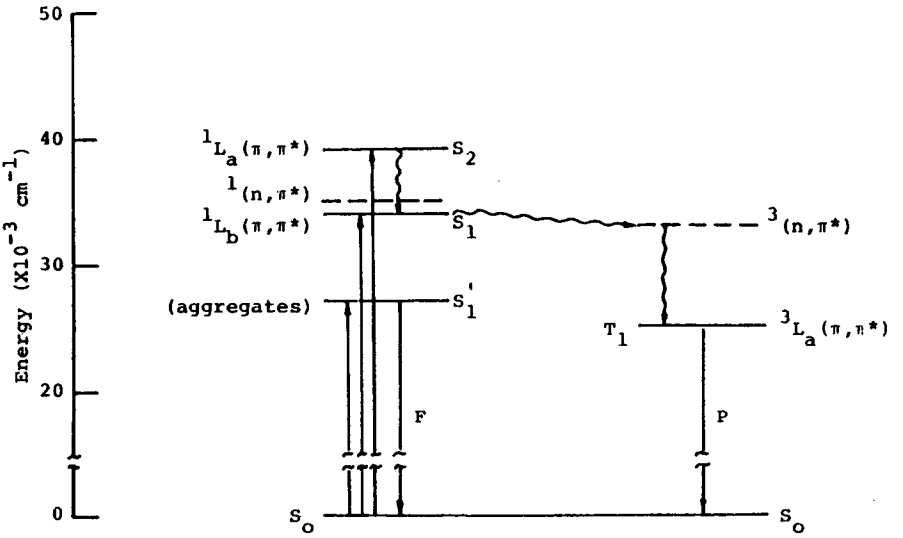

Fig. 7. Electronic energy level diagram and transitions for poly(ethylene terephthalate). Estimated levels are represented by broken lines.

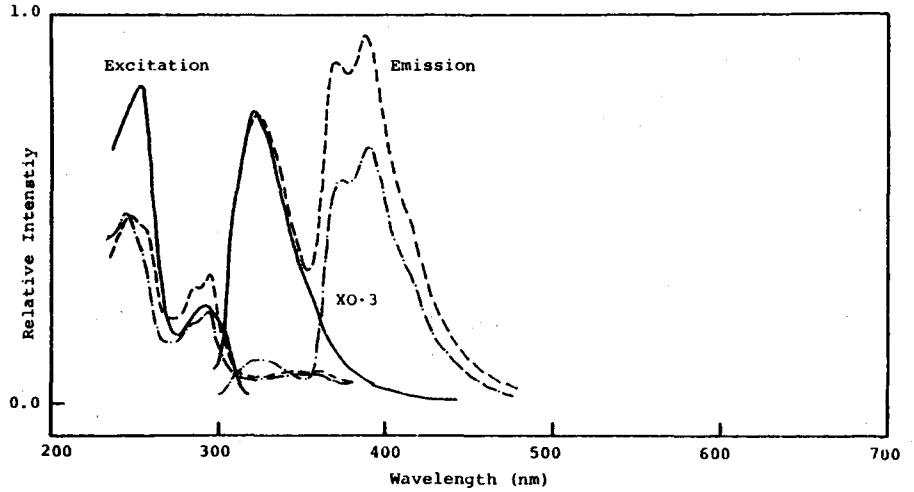

Fig. 8. Corrected fluorescence excitation and emission spectra for poly(ethylene terephthalate-*co*-2,6-naphthalenedicarboxylate) in HFIP. Excitation scan: Em λ 388 nm; emission scan: Ex λ 294 nm; (- - -) 1 mol % 2,6-DMN; (-·-) 4 mol % 2,6-DMN; (—) PET; excitation scan: Em λ 324 nm; emission scan: Ex λ 294 nm.

excitation bands were observed at about 290 and 325–360 nm, and the emission spectra show an emission band centered at about 385 nm. The relative fluorescence quantum yields from terephthalate and naphthalenedicarboxylate units in the solid copolymers are evident. Even at 0.5 mol % 2,6-DMN, the naphthalenedicarboxylate comonomer completely dominates the fluorescence emission from the copolymer yarn. Only the emission at about 385 nm was observed and the emission intensity is at least 30 times greater than that of the PET itself.

Figure 10 presents some of the phosphorescence spectra of the copolymer yarns. Excitation band maxima were observed at 298, 312, and 354 nm, and the

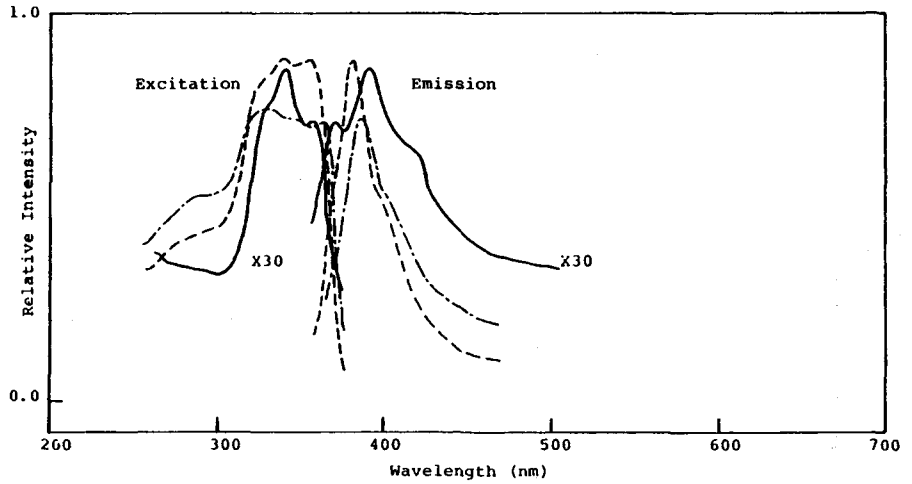

Fig. 9. Corrected fluorescence excitation and emission spectra of poly(ethylene terephthalate-*co*-2,6-naphthalenedicarboxylate) yarns. Excitation scan: Em λ 380 nm; emission scan: Ex λ 360 nm; (- - -) 1 mol % 2,6-DMN; (-·-) 4 mol % 2,6-DMN; (—) PET yarn; excitation scan: Em λ 390 nm; emission scan: Ex λ 342 nm.

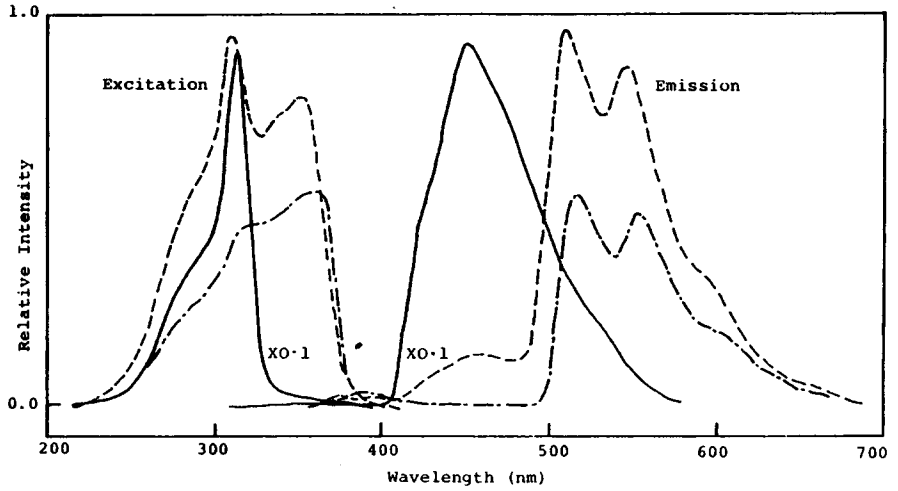

Fig. 10. Uncorrected phosphorescence excitation and emission spectra of poly(ethylene terephthalate–*co*–2,6-naphthalendicarboxylate) yarns. Excitation scan: Em λ 510 nm; emission scan: Ex λ 312 nm; (- - -) 1 mol % 2,6-DMN; (- · -) 4 mol % 2,6-DMN; (——) PET yarn; excitation scan: Em λ 452 nm; emission scan: Ex λ 312 nm.

emission spectra show peak maxima at about 385, 456, 507–515, and 546–554 nm. The emission band at 456 nm corresponds to the PET phosphorescence originating from the terephthaloyl units. This emission band decreases in intensity with increasing 2,6-DMN concentration, and at 2.0 mol % 2,6-DMN practically no emission at 456 nm was observed from the copolymer yarn.

The emission system of the copolymer starting at 507 nm corresponds to the 2,6-DMN monomer phosphorescence. The excitation spectrum reveals that two excitation systems are responsible for the emission bands at 510 and 540 nm. The excitation at 354 nm originates from the naphthalenedicarboxylate moieties in the copolymer. Part of the excitation radiation at 312 nm results in excitation of the naphthalenedicarboxylate moieties to their second excited singlet state, but the major part of the excitation radiation at 312 nm is first absorbed by the terephthalate units, and through triplet–triplet energy transfer process the excitation energy is transferred to the triplet state of the naphthalenedicarboxylate moiety; this results in a sensitized phosphorescence.

Because the naphthalendicarboxylate monomer absorbs at the same spectral region as the terephthalate moiety, selective excitation of the terephthalate units is not possible. However, it has been shown that the fluorescence emission of the copolymer yarn at about 380 nm originates solely from the naphthalenedicarboxylate monomer. Thus, the low-temperature fluorescence excitation spectrum of the copolymer yarn monitored at the 380 nm emission will also show the phosphorescence excitation spectra of the naphthalenedicarboxylate monomer at 77°K. The amount of sensitized phosphorescence emission at 510 nm resulting from triplet–triplet energy transfer can be estimated by comparing the low-temperature fluorescence excitation spectra of the copolymer yarn with emission monitored at 380 nm and the phosphorescence excitation spectrum with emission monitored at 510 nm (Fig. 11). The results show that in the copolymer yarn containing 0.5 mol % 2,6-DMN, about 75% of the phosphorescence emission at 510 nm arises from the triplet–triplet energy transfer process when the excitation radiation is at 312 nm.

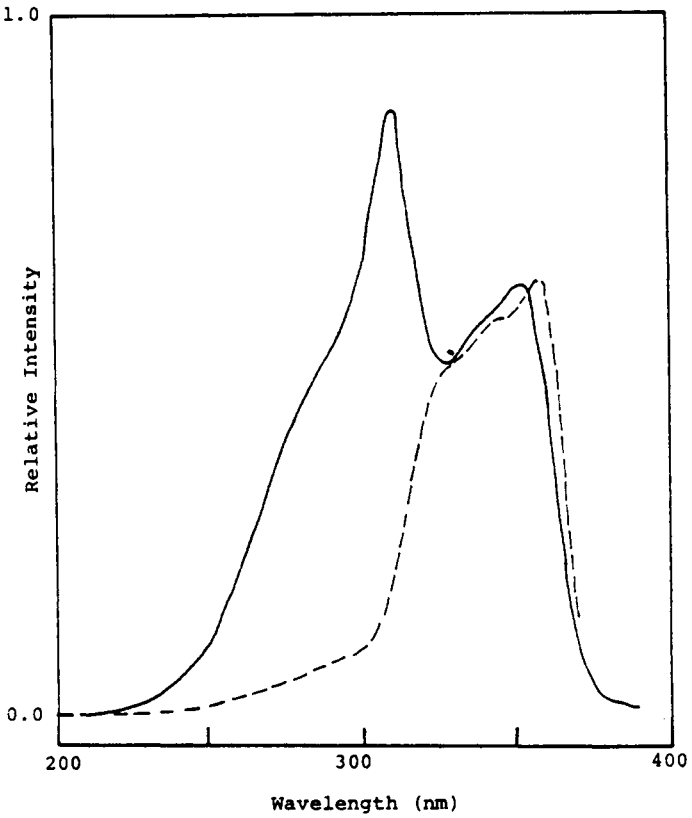

Fig. 11. Uncorrected low-temperature excitation spectra of poly(ethylene terephthalate–*co*–2,6-naphthalenedicarboxylate) yarn; 0.5 mol % 2,6-DMN, at 77°K. (——) Phosphorescence excitation scan: Em λ 510 nm; (- - -) low-temperature fluorescence excitation scan: Em λ 380 nm.

The quenching of PET phosphorescence at 456 nm and simultaneous sensitized phosphorescence at 510 nm conform the presence of a triplet–triplet transfer process in the copolymer when excited at 312 nm. Under constant irradiation condition at 312 nm, the following reactions are considered to be involved:

$^1PET + h\nu \rightarrow {}^1PET^*$	absorption
$^1ND + h\nu \rightarrow {}^1ND^*$	absorption
$^1PET^* \rightarrow {}^3PET^*$	intersystem crossing
$^1ND^* \rightarrow {}^3ND^*$	intersystem crossing
$^3PET^* \rightarrow {}^1PET + h\nu'$	PET phosphorescence
$^3ND^* \rightarrow {}^1ND + h\nu''$	ND phosphorescence
$^3PET+ + {}^1ND \rightarrow {}^1PET + {}^3ND^*$	T–T energy transfer
$^3ND^* \rightarrow {}^1ND + h\nu''$	ND-sensitized phosphorescence

The triplet–triplet energy transfer, while forbidden by the long-range dipole–dipole radiationless transfer mechanism, is allowed by the electron exchange

mechanism. By applying the method of Inokuti and Hirayama,[59] the energy transfer process was shown to proceed by an exchange mechanism and is approaching that of the Perrin model.

The quenching of phosphorescence of the donor as a function of acceptor concentration has been described by Perrin[60] as

$$\phi/\phi_0 = \exp(VNC_A)$$

where ϕ_0 and ϕ are phosphorescence quantum yield of the donor in the absence and presence of the acceptor, respectively; V is the volume of the quenching sphere; C_A is the concentration of the acceptor, in mol/l.; and N is Avogadro's number.

From the intensity data at 456 nm, a Perrin plot was constructed. A quenching sphere of 3.22×10^{-20} cm^3 and a critical transfer radius, R_0 = 19.7 Å, were computed from the data. A critical concentration, $C_0 = 5.2 \times 10^{-2}$ mol/l., was calculated from the relation $C_0 = 3000/4NR_0^3$ mol/l. This critical concentration corresponds to 0.8 mol % 2,6-DMN in the copolymer where over 95% of the PET phosphorescence at 456 nm was quenched.

The value of R_0, 19.7 Å, measured in the PET–2,6-ND system is greater than the normal critical transfer distance, ~15 Å, allowed by exchange mechanism, which requires direct contact between donor and acceptor. Hence, energy migration must be operative in the copolymer; and this has been observed in many polymer systems.[25,27,31]

Since the lowest excited singlet of the 2,6-ND moiety in the polymer lies at a lower energy level than that of the PET unit, there is a possibility of singlet–singlet energy transfer from the PET units to the 2,6-ND units. The presence of singlet–singlet energy transfer would result in quenching of PET fluorescence and sensitization of 2,6-ND monomer fluorescence. The relative emission intensities at 325 nm (due to PET fluorescence) of the copolyester in HFIP solution with excitation at 294 nm is shown in Table IV. The slight decrease in the PET fluorescence at high concentrations of 2,6-ND monomer is probably due to the competition of incident radiation absorption by the comonomer rather than to the quenching of fluorescence by singlet–singlet energy transfer. By comparing the relative fluorescence and phosphorescence quenching of PET in the presence of 2,6-ND monomer (Table IV), it appears that the singlet–singlet energy transfer process would be of minor importance, even if it exists as compared to triplet–triplet energy transfer, which results in dramatic phosphorescence quenching. Since no delayed fluorescence was observed from the PET homopolymer, it is

TABLE IV
Fluorescence Quenching of Poly(ethylene Terephthalate–*co*–2,6-Naphthalenedicarboxylate) in Hexafluoroisopropanol and Phosphorescence Quenching of the Copolymer in Filament Yarns

2,6-DMN, mol %	Relative emission intensity	
	Fluorescence 325 nm	Phosphorescence 452 nm
0.0	1.0	1.0
0.5	0.98	0.034
1.0	0.93	0.014
2.0	0.88	0.003
4.0	0.80	~0

unlikely that the delayed emission band at 385 nm observed in the copolymer originates from the PET units. It appears that the delayed emission at 385 nm is the delayed fluorescence from the naphthalenedicarboxylate monomer units and results from triplet–triplet annihilation processes. Since excitation at 310 nm would excite both the PET and 2,6-ND units in the copolymer, the following reactions are probably involved in the delayed fluorescence process:

$^3PET^* + {}^3ND^* \rightarrow PET_0 + {}^1ND^*$	T–T annihilation
$^3ND^* + {}^3ND^* \rightarrow ND_0 + {}^1ND^*$	T–T annihilation
$^1ND^* \rightarrow ND_0 + h\nu$	delayed fluorescence

Unfortunately, the intensity of the delayed emission at 385 nm was too weak to render lifetime measurements and further analysis. The electronic transitions, band assignments, and energy transfer processes in the copolymer system are shown in Figure 12.

Phototendering of PET and PET–2,6-ND Filament Yarns

The series of PET–2,6-ND copolymer filament yarns containing 0.5–4.0 mol % DMN monomer together with the homopolymer PET filament yarn were irradiated from 20 to 80 hr in the photolysis chamber. The variation of incident light intensity during the photolysis period was taken into consideration when plotting the phototendering rate curve, where the percent loss in yarn breaking strength was expressed as a function of total incident quanta absorbed rather than as a function of irradiation time.

The phototendering rate curves for PET homopolymer and PET–2,6-ND copolymer yarns are shown in Figure 13. All yarn samples became weaker and more brittle and showed lower percent elongation at break with increasing irradiation times. The results show that the yarn samples can be divided into two groups: Yarn samples containing 0.0, 0.5, and 1.0 mol % 2,6-DMN monomer belong to the first group where the rate of phototendering was fast, and yarn samples containing 2.0 and 4.0 mol % 2,6-DMN monomer belong to the second group where the rate of phototendering was slow.

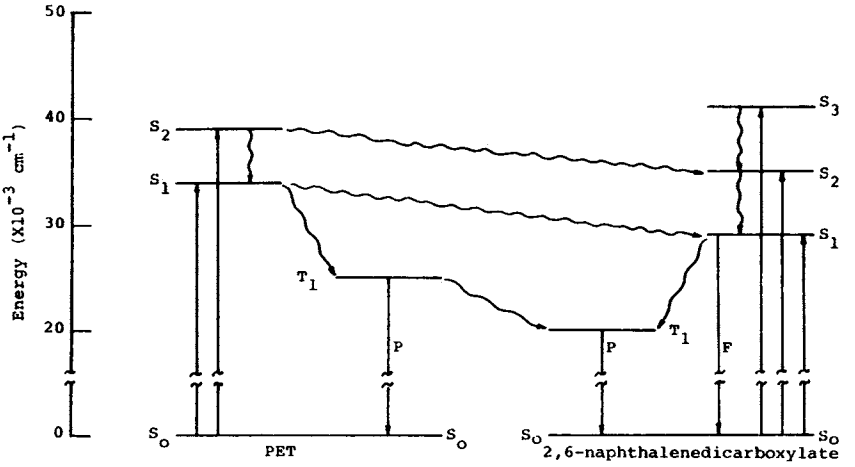

Fig. 12. Electronic energy level diagram and transitions for poly(ethylene terephthalate–*co*–2,6-naphthalenedicarboxylate) yarn.

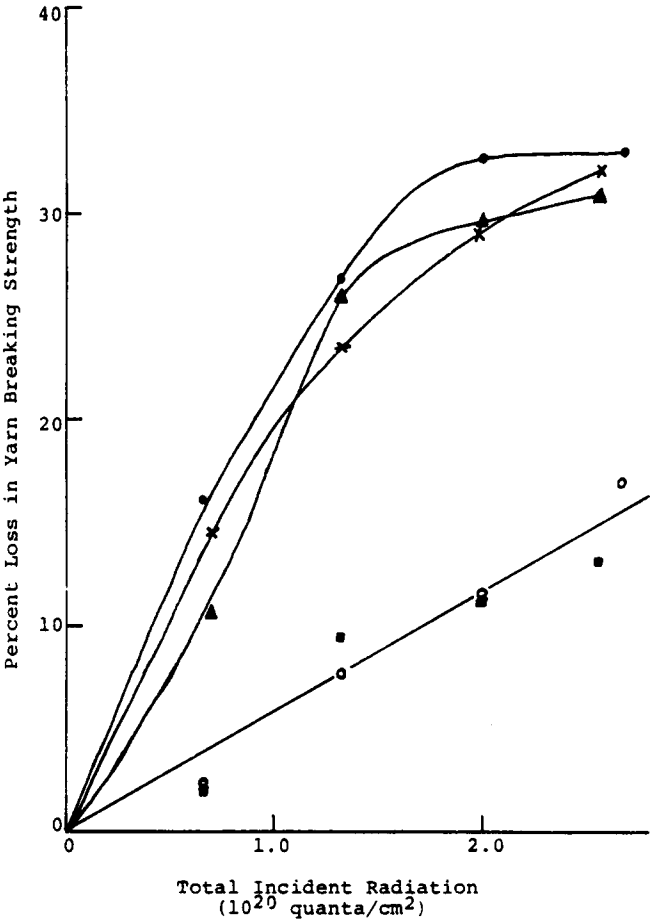

Fig. 13. Effect of radiation on the poly(ethylene terephthalate–*co*–2,6-naphthalenedicarboxylate) yarns. Mol % of 2,6-DMN: (●) 0.0; (X) 0.5; (▲) 1.0; (○) 2.0; (■) 4.0.

Assuming a zero-order rate of phototendering of yarn samples at the initial stage of photolysis and using a least-squares analysis gave a phototendering rate constant for the yarn samples in the first group of $k_1 = 2.0 \times 10^{-19}$% breaking strength loss/quantum absorbed/cm^2, and a phototendering rate constant for, the second group $K_2 = 0.7 \times 10^{19}$% breaking strength loss/quantum absorbed/cm^2. The phototenderizing rate constant for the yarn samples in the first group agrees with the result reported by Merrill and Roberts[10] for PET homopolymer.

From the kinetic analysis and the relative quantum yields of CO_2 and —COOH endgroups in photolysis of PET, Day and Wiles[13] showed the importance of the Norrish type II intramolecular rearrangement reaction in the PET photodegradation mechanisms. It has been shown that both the lowest excited singlet and triplet states can be involved in the Norrish type II cleavage of alkyl ketones.[61,62] In the present luminescence and tensile studies in PET and PET–2,6-ND yarns, the amount of 2,6-DMN monomer (2.0 mol %) in the copolymer yarn which gives the ultimate quenching of the PET phosphorescence also reduces the rate of phototendering to one third of that in homopolymer PET. This

shows that the lowest excited triplet in PET plays an important role in the photodegradation processes of the polymer and that the Norrish type II rearrangement process in PET photodegradation mechanisms probably involves the triplet state.

Fluorescence Analysis of Irradiated PET and PET–2,6-ND Yarns

An emission band at 460 nm was observed in the irradiated PET yarn. The observance of a blue-green fluorescence material on irradiated PET polymer has been reported.[8,11] The monohydroxy terephthaloyl compound was found to be responsible for the emission band[8] at 460 nm. The fluorescence emission spectrum of the irradiated PET–2,6-ND yarn is similar to that of the unirradiated sample but with lower emission intensity. The decrease in fluorescence intensity for the irradiated copolymer sample is probably due to the absorption of excitation radiation by the photo-oxidized materials formed at the surface of the copolymer. The fluorescence emission at 460 nm that was observed in irradiated PET samples was not observed in the copolymer yarns. It appears that the weak 460 nm emission band is probably hidden under the intense emission band at 384 nm that originated from the naphthalenedicarboxylate units.

CONCLUSIONS

The phototendering studies of poly(ethylene terephthalate) and poly(ethylene terephthalate–*co*–2,6-naphthalenedicarboxylate) yarns reveal that photostabilization of PET can be obtained through copolymerization with dimethyl 2,6-naphthalenedicarboxylate at about 2 mol % concentration. Kinetic analysis of the phototendering data indicates a decrease of phototendering rate from 2.0 $\times 10^{-19}$% breaking strength loss/quantum absorbed/cm^2 to 0.7 $\times 10^{-19}$% breaking strength loss/quantum absorbed/cm^2. From luminescence studies, quenching of PET phosphorescence with simultaneous sensitization of 2,6-ND phosphorescence indicates that triplet–triplet energy transfer is involved in the copolymer system. A kinetic analysis of the transfer process shows that the energy transfer mechanism involves electron exchange interaction; a critical transfer distance R_0 of 19.7 Å was computed, and energy migration is believed to occur during the energy transfer process.

The fluorescence and phosphorescence properties of monomers DMT and 2,6-DMN have been studied. The results show that the lowest excited single and triplet in both monomers are of the $^1(\pi,\pi^*)$ and $^3(\pi,\pi^*)$ types, respectively.

The luminescence characteristics of PET have been examined and the corresponding electronic transitions are tentatively assigned. The emitting triplet state of PET is identified as a $^3(\pi,\pi^*)$ state, and the excited triplets are involved in the photodegradation of PET. Although the exact nature of the luminescent chromophore for the fluorescence emission at 390 nm is uncertain, it is believed that the emission may arise from oriented aggregates in the PET polymer matrix and can be explained as a crystal effect.

The delayed emission at 385 nm observed in the copolymer at 77°K is probably due to the delayed fluorescence from the 2,6-ND units through triplet–triplet annihilation processes.

The blue-green fluorescence observed in the irradiated PET yarn possibly originates from the monohydroxy terephthaloyl units which are formed during the photo-oxidative process. The decrease of fluorescence intensity at 380 nm in irradiated copolymer yarns is probably due to the absorption of excitation radiation by the photo-oxidatized materials formed at the surface of the copolymer yarns.

The authors would like to thank Mr. Ron Worley (American Enka Company) for his technical assistance in polymer synthesis. This manuscript was taken from a dissertation submitted by P.S.R. Cheung to Clemson University in partial fulfillment of the requirements for the degree of Doctor of Philosophy in Chemistry, August 1978.

References

1. F. B. Marcotte, D. Campbell, and J. A. Cleaveland, *J. Polym. Sci. Part A-I,* **5**, 481 (1967).
2. C. V. Stephenson and W. S. Wilcox, *J. Polym. Sci. Part A-I,* **1**, 2741 (1963).
3. T. Matsuda and F. Kurihara, *Chem. High Polym. Jpn.,* **22,** 435 (1965).
4. M. J. Wall and G. C. Frank, *Text. Res. J.,* **41,** 32 (1971).
5. K. R. Osborne, *J. Polym. Sci.,* **38,** 357 (1959).
6. C. V. Stephenson, B. C. Moses, and W. S. Wilcox, *J. Polym. Sci.,* **55,** 451 (1961).
7. G. Valk, M. L. Kehren, and I. Daamen, *Angew. Makromol. Chem.,* **13,** 97 (1970).
8. J. G. Pacifici and J. M. Straley, *J. Polym. Sci., Polym. Lett. Ed.,* **7**, 7 (1969).
9. D. Campbell, L. K. Monteith, and D. T. Turner, *J. Polym. Sci. Part A-I,* **8**, 2703 (1970).
10. R. G. Merrill and C. W. Roberts, *J. Appl. Polym. Sci.,* **21,** 2745 (1977).
11. M. Day and D. M. Wiles, *J. Appl. Polym. Sci.,* **16,** 175 (1972).
12. M. Day and D. M. Wiles, *J. Appl. Polym. Sci.,* **16,** 191 (1972).
13. M. Day and D. M. Wiles, *J. Appl. Polym. Sci.,* **16,** 203 (1972).
14. P. Blais, M. Day, and D. M. Wiles, *J. Appl. Polym. Sci.,* **17,** 1895 (1973).
15. J. D. Jackson, *Classical Electrodynamics,* Wiley, New York, 1962, Chap. 4.
16. J. Perrin, *Compt. Rend.,* **184,** 1097 (1927).
17. T. Forster, *Naturwissenschaften* **33,** 166 (1946).
18. T. Forster, *Ann. Phys.,* **2,** 55 (1948).
19. T. Forster, *Fluoreszenz Organischer Verbindungen,* Vandenhoeck and Ruprecht, Gottingen, 1951.
20. D. L. Dexter, *J. Chem. Phys.,* **21,** 836 (1953).
21. F. Wilkinson, in *Advances in Photochemistry,* Vol. III, W. A. Noyes, G. S. Hammond, and J. N. Pitts, Jr., Eds., Interscience, New York, 1964, p. 241.
22. G. Porter and M. R. Wright, *Discuss. Faraday Soc.,* **27,** 18 (1959).
23. J. Frenkel, *Phys. Rev.,* **37,** 1276 (1931).
24. A. S. Davydov, *Theory of Molecular Exciton* (translated by M. Kasha and M. Oppenheimer), McGraw-Hill, New York, 1962.
25. C. David, W. Demarteau, and G. Geuskens, *Eur. Polym. J.,* **6**, 537 (1970).
26. C. David, W. Demarteau, and G. Geuskens, *Eur. Polym. J.,* **6**, 1397 (1970).
27. C. David, W. Demarteau, and G. Geuskens, *Eur. Polym. J.,* **6**, 1405 (1970).
28. C. David, N. Putnam, M. Lempereur, and G. Geuskens, *Eur. Polym. J.,* **8**, 409 (1972).
29. C. David, M. Lempereur, and G. Geuskens, *Eur. Polym. J.,* **8**, 417 (1972).
30. C. David, M. Piens,and G. Geuskens, *Eur. Polym. J.,* **9**, 533 (1973).
31. C. David, V. Naegelen, W. Piret, and G. Geuskens, *Eur. Polym. J.,* **11,** 569 (1975).
32. N. J. Turro, *Pure Appl. Chem.,* **49,** 405 (1977).
33. J. E. Guillet, *Pure Appl. Chem.,* **49,** 249 (1977).
34. B. Ranby and J. F. Rabek, *Photodegradation, Photooxidation and Photostabilization of Polymers,* Interscience, New York, 1975.
35. R. S. Becker, *Theory and Interpretation of Fluorescence and Phosphorescence,* Interscience, New York, 1969.
36. J. B. Birks, *Photophysics of Aromatic Molecules,* Interscience, New York, 1970.
37. P. S. R. Cheung, Master's Thesis, Clemson University, December 1974.
38. N. S. Allen and J. F. McKellar, *Makromol. Chem.,* **179,** 523 (1978).
39. H. A. Pohl, *Anal. Chem.,* **26,** 1614 (1954).

40. C. A. Parker, *Proc. R. Soc. London Ser. A,* **A220,** 104 (1953).
41. C. G. Hatchard and C. A. Parker, *Proc. R. Soc. London Ser. A,* **A235,** 518 (1956).
42. J. H. Baxendale, N. K. Bridge, *J. Phys. Chem.,* **59,** 783 (1955).
43. J. Lee and H. Selinger, *J. Chem., Phys.,* **40,** 519 (1964).
44. K. C. Kurien, *J. Chem. Soc. B,* **No. 10,** 2081 (1971).
45. D. E. Nicodem, M. L. P. F. Cabral, and J. C. N. Ferreira, *Mol. Photochem.,* **8** (3), 213 (1977).
46. H. Baba and M. Kitamura, *J. Mol. Spectrosc.,* **41,** 302 (1972).
47. R. N. Nurmukhametov and G. I. Grishina, *Opt. Spectrosc.,* **24,** 107 (1968).
48. R. M. Silverstien, G. C. Bassler, and T. C. Morrill, *Spectrometric Identification of Organic Compounds,* Wiley, New York, 1974.
49. M. A. El-Sayed, *J. Chem., Phys.,* **38,** 2834 (1963).
50. D. H. Phillips and J. C. Schug, *J. Chem. Phys.,* **50,** 3297 (1967).
51. R. M. Hochstrasser, *Can. J. Chem.,* **39,** 1776 (1961).
52. R. M. Hochstrasser, *Can. J. Chem.,* **39,** 1853 (1961).
53. I. L. Belaits, R. N. Nurmukhametov, and D. N. Shigorin, *Russ. J. Phys. Chem.,* **43** (4), 480 (1969).
54. C. J. Seliskar, O. S. Khalil, and S. P. McGlynn, Luminescence Characteristics of Polar Aromatic Molecules, in *Excited States,* E. C. Lim, Ed., Academic Press, New York, 1975, p. 252.
55. Y. Takai, T. Osawa, T. Mizutani, and M. Ieda, *J. Polym. Sci., Polym. Phys. Ed.,* **15,** 945 (1977).
56. N. S. Allen, J. Homer, and J. F. McKellar, *Analyst,* **101,** 260 (1976).
57. M. R. Padhyde and P. S. Tamhane, *Angew. Makromol. Chem.,* **69,** 33 (1978).
58. Y. Takai, T. Mizutani, and M. Ieda, *Jpn. J. Appl. Phys.,* **17,** 651 (1978).
59. M. Inokuti and F. Hirayama, *J. Chem. Phys.,* **43,** 1978 (1965).
60. F. Perrin, *Compt. Rend.,* **178,** 1978 (1924).
61. P. J. Wagner and G. S. Hammond, *J. Am. Chem. Soc.,* **87,** 4009 (1965).
62. T. J. Doughterty, *J. Am. Chem. Soc.,* **87,** 4011 (1965).

Received December 22, 1978
Revised May 15, 1979